Dynamical Modeling of Coupled Orbit-Attitude Motion of a Rigid Body in the Gravity of an Asteroid Considered as a Polyhedron

Yue Wang [1], Yu Shi [2], Shijie Xu [3]

[1] School of Astronautics, Beihang University, 37 Xueyuan Road, Haidian District, Beijing, 100083, China
[2] School of Astronautics, Beihang University, 37 Xueyuan Road, Haidian District, Beijing, 100083, China
[3] School of Astronautics, Beihang University, 37 Xueyuan Road, Haidian District, Beijing, 100083, China

Abstract

For spacecraft about small asteroids, the gravitational orbit-attitude coupling effect becomes much more significant than orbiting large celestial bodies, due to the large ratio of the spacecraft dimension to the orbit radius. To model the spacecraft motion more precisely, the 6-DOF, coupled orbit-attitude dynamics have been proposed, in which the spacecraft is modeled as a rigid body rather than a point mass. Existing coupled orbit-attitude dynamical models have used harmonic series to describe the gravity field of the asteroid. However, harmonic series diverges near and inside the circumscribing sphere of the asteroid, causing large errors near the asteroid's surface. In this paper, a new model for the gravitationally coupled orbit-attitude dynamics about an asteroid is established, with the gravity field modelled as that of a homogeneous polyhedron, so that the irregular gravity field can be fully modelled without discarding higher-order terms, enabling a high precision even near the asteroid's surface. By using Taylor expansion, the potential, formulated as a volume integral over the spacecraft, is rewritten in terms of inertia integrals of the spacecraft and truncated on the second-order, i.e., the moments of inertia, which is precise enough for our purpose. The gravitational force and torque are derived by means of derivatives of the potential. The proposed model is compared with models with the point-mass/spherical gravity and the harmonic gravity, to see effects of irregularity of the asteroid's shape. Results show that the irregularity of the gravity has significant effects on the coupled orbit-attitude dynamical model, and cannot be precisely described by harmonic series. The proposed model with the gravity of a homogeneous polyhedron provides a high-precision description for the coupled orbit-attitude motion in the close proximity of a small, irregular-shaped asteroid.

Keywords: Irregular-shaped asteroid, Homogeneous polyhedron, Extended body, Coupled orbit-attitude dynamics, Gravitational potential, force, and torque

Introduction

The orbit-attitude motion of a rigid body in a gravity of another rigid body is quite common in celestial mechanics, such as in the dynamical evolution of binary asteroids, usually referred as the Full Two Body Problem (F2BP) [1]-[13]. Because of the asteroids' non-spherical shapes and the proximity in distance, their rotational and translational motions are coupled significantly through the mutual gravitational potential. The gravitational orbit-attitude coupling effects and the related gravitationally coupled orbit-attitude dynamics are distinct from the classical, uncoupled orbital and attitude motions.

To investigate the dynamical evolution of binary asteroids, various gravitational models, including the gravitational potential, force, and torque, have been proposed. The basic form of

the mutual gravitational potential is a double volume integration of reciprocal distance between mutual mass elements over both bodies. The usual approach is expanding the potential in an asymptotic series in terms of ratio of body sizes over the distance. The asymptotic series is then rearranged further in terms of different types of mass distribution parameters of the two bodies, including inertia integrals [5],[8],[11],[12],[14]-[16], spherical harmonics [17]-[19], mass distribution parameters derived from shapes of homogeneous polyhedra [20]-[23], and the symmetric trace free (STF) tensor of homogeneous polyhedra [24]. These different types of mass distribution parameters are actually the same kind of physical parameters of the body and play the same role in the formulation of gravity [16],[24]. In practice, these approaches all discarded higher-order terms for both the two bodies.

Recently, the authors have proposed a novel shaped-based approach to model mutual potential of two asteroids of a binary system [25]. One asteroid is modeled as a homogeneous polyhedron and its gravity is described in a closed form via the approach by Werner and Scheeres [26], while the other one is modeled as an extended body. The mutual potential is formulated as a volume integral over the extended body, and, then, as a Taylor series in terms of its inertia integrals. Unlike previous gravitational models, this model can take into account the irregular shape of the polyhedral asteroid exactly without discarding higher-order terms.

With the coming of the space age, early pioneers of astrodynamics and spaceflight dynamics have investigate gravitationally coupled orbit-attitude dynamics and orbit-attitude coupling effects for Earth-orbiting artificial satellites that are modeled as extended bodies. They have found that the gravitational orbit-attitude coupling is quite weak and then negligible, due to the extremely small ratio of the spacecraft dimension to the orbit radius, being order of 10^{-6} or even smaller [27]-[31]. From then on, the gravitational orbit-attitude coupling has always been regarded to be negligible in spaceflight dynamics, and the community has taken the uncoupled orbit and attitude dynamics for granted. It has become axiomatic, common sense that the spacecraft is first treated as a point mass in the orbital dynamics, and the attitude motion is then treated as a restricted problem on the predetermined orbit. Consequently, the orbit motion of the spacecraft is not affected by its attitude motion.

However, the situation has been different as the human's space activities extend to the close proximity of small celestial bodies, i.e., asteroids and comets. In the close proximity of a small asteroid, due to the large ratio of the spacecraft dimension to the orbit radius, a significant gravitational coupling can exist between the orbit and attitude motions of a large spacecraft, as shown by Wang and Xu [32]. The magnitude of gravitational orbit-attitude coupling can be estimated by $\varepsilon = \rho / r_0$, where ρ is the spacecraft's characteristic dimension and r_0 is the orbital radius [30]. For a spacecraft in a 1 km-sized orbit about a small asteroid, ε can be order of 10^{-2}, much larger than the value about Earth. The precision of traditional spacecraft dynamics, in which the orbit and attitude motions are regarded to be uncoupled and are modelled separately, will degenerate in the close proximity of small asteroids due to the significant gravitational orbit-attitude coupling [32],[33].

For this reason, in recent years, the gravitationally coupled orbit-attitude dynamics, which have been almost forgotten in the field of spaceflight dynamics, have been experiencing a renaissance in the spaceflight dynamics about asteroids, where it can be also called the full dynamics as the spacecraft is modeled as an extended, rigid body. The gravitationally coupled orbit-attitude dynamics of spacecraft has been studied qualitatively in a J_2-truncated gravity field of a small spheroid asteroid [34]-[36] and in the second degree and order gravity field of a uniformly rotating asteroid with the harmonic coefficients C_{20} and C_{22} [37],[38]. Although

the higher-order harmonic coefficient J_4 has been considered by Wang and Xu [32] and Kikuchi et al. [39], the coefficient J_4 is only included in the point-mass potential but not in the extended-body potential, having no contribution to the gravitational coupling terms. The gravitationally coupled orbit-attitude dynamics of spacecraft already have some applications in the control and navigation of the asteroid close-proximity operations [40]-[42].

The gravitationally coupled orbit-attitude dynamics about an asteroid is actually a restricted problem of the F2BP. That is, only the motion of the spacecraft is considered and the motion of the asteroid is assumed to be not affected by the spacecraft. The derivation of equations of motion for a rigid body is a classical problem, which can be addressed well by using the Newton-Euler method, and also can be addressed via the non-canonical Hamiltonian structure of the problem [43]. One of the advantages of the non-canonical Hamiltonian approach is that it naturally provides expressions for the gravitational force and torque in terms of derivatives of the potential. Since the equations of motion are already known and the gravitational force and torque can be derived from the potential, the essential problem in the dynamical modeling of gravitationally coupled orbit-attitude motion is how to model the potential of the extended, rigid body in the irregular gravity of the asteroid, which is the same with the essential problem in the dynamical modeling of F2BP.

As for modeling the potential of a rigid body in the gravity of an asteroid, existing coupled orbit-attitude dynamical models have used the harmonic expansion to represent the irregular gravity of the asteroid, including the J_2 model [34]-[36], the J_2-J_4 model [32], the C_{20}-C_{22} model [37][38], and the C_{20}-C_{22}-J_4 model [39]. However, the harmonic series diverges near and inside the circumscribing sphere of the asteroid, causing large errors near its surface. Thus, the harmonic series cannot represent the highly irregular gravity in the close proximity of the asteroid, where the spacecraft is usually required to be during in-situ explorations and the surface sampling. Although it is helpful to employ a higher-degree harmonic series, the improvement on the precision is limited near the asteroid surface, and the cost will be large, because of the rapid-increasing amount of terms in the potential formulation [39].

Actually, the various gravitational models proposed for F2BP mentioned before can be used to model the potential of the extended spacecraft in the gravity of the asteroid, just replacing one asteroid with the spacecraft. However, as stated before, most of gravitational models of F2BP have adopted two bodies' mass distribution parameters that are equivalent to spherical harmonics. Thus, they have same drawbacks with existing dynamical models with harmonic gravities, that is, cannot represent the gravity precisely near the surface of irregular-shaped asteroid. This drawback is not a problem in F2BP, since the asteroids usually move far away from each other's circumscribing sphere. However, it is not the case for spacecraft executing asteroid close-proximity operations.

Fortunately, the shaped-based model for mutual potential of two asteroids by us [25] provides a promising method for modeling the potential of an extended spacecraft in the irregular gravity of an asteroid. In this approach, the asteroid is modeled as a homogeneous polyhedron, and, thus, its irregular gravity can be described exactly without discarding higher-order terms, having a high precision even near the surface. The spacecraft is modeled as an extended, rigid body, and only the inertia integrals up to the second-order, i.e., moments of inertia, need to be taken into account for our purpose. In the end, the potential of the spacecraft has a closed, compact form, and is easy to implement.

In this study, a new gravitationally coupled orbit-attitude dynamical model for an extended, rigid spacecraft about an irregular-shaped asteroid will be established with our approach in

Ref. [25]. The 6-DOF, gravitationally coupled orbit-attitude motion of the spacecraft is numerically propagated and compared with different gravity models of the asteroid, including harmonic gravity and point-mass/spherical gravity, to show dynamical effects of irregularity of gravity. Results show that the proposed coupled orbit-attitude dynamics provide a high-precision model for spacecraft in the close proximity of a small, irregular-shaped asteroid, and are of great significance for studies in related areas.

Equations of Coupled Orbit-Attitude Motion

As shown in Fig. 1, the spacecraft *B*, modeled as an extended, rigid body, is moving about a uniformly rotating asteroid *P*, the gravity of which is modeled as that of a homogeneous polyhedron. We have chosen principal-axis body-fixed reference frames for the asteroid and the spacecraft, $S_P=\{\boldsymbol{u}, \boldsymbol{v}, \boldsymbol{w}\}$ and $S_B=\{\boldsymbol{i}, \boldsymbol{j}, \boldsymbol{k}\}$ with origins *O* and *C* at the centers of mass, respectively. It is assumed that the center of mass of the asteroid is stationary in the inertial space, and the asteroid is rotating uniformly around its maximum-moment principal axis, ***w***-axis, with the angular velocity ω_T.

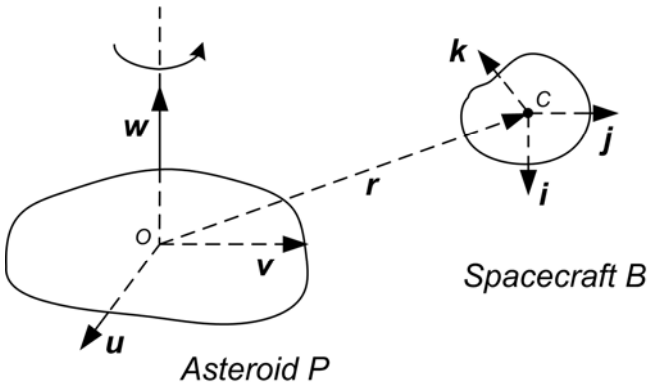

Fig. 1: The spacecraft B, modeled as an extended, rigid body in the vicinity of the asteroid P, which is modeled as a homogeneous polyhedron

The attitude of the spacecraft is described with respect to the asteroid body-fixed frame S_P by

$$\boldsymbol{A}=[\boldsymbol{\alpha}_a, \boldsymbol{\beta}_a, \boldsymbol{\gamma}_a] \in SO(3), \tag{1}$$

where $\boldsymbol{\alpha}_a$, $\boldsymbol{\beta}_a$, and $\boldsymbol{\gamma}_a$ are coordinates of unit vectors ***i***, ***j***, and ***k*** of the spacecraft frame S_B expressed in the asteroid frame S_P, respectively. The position vector of the spacecraft's center of mass *C* with respect to the asteroid's center of mass *O* expressed in the asteroid frame S_P is denoted by $\boldsymbol{r}=[r^x, r^y, r^z]^T$, and the unit vector along ***r*** is denoted by $\bar{\boldsymbol{r}}=[\bar{r}^x, \bar{r}^y, \bar{r}^z]^T$. The configuration space of the problem is Lie group $Q=SE(3)$, known as the special Euclidean group with elements $(\boldsymbol{A}, \boldsymbol{r})$, which is the semidirect product of $SO(3)$ and $\mathbb{R}^3$. Accordingly, the (momentum) phase space of the problem is the cotangent bundle T^*Q.

As in Ref. [43], we choose coordinates for the phase space as

$$\boldsymbol{z}=\left[\boldsymbol{\Gamma}^T, \boldsymbol{\alpha}_a^T, \boldsymbol{\beta}_a^T, \boldsymbol{\gamma}_a^T, \boldsymbol{r}^T, \boldsymbol{p}^T\right]^T \in \mathbb{R}^{18}, \tag{2}$$

where $\boldsymbol{\Gamma}$ and $\boldsymbol{p}$ are the angular momentum and linear momentum of the spacecraft expressed in the asteroid frame S_P, respectively. $\boldsymbol{z}$ has been called inertial coordinates in Ref. [43], but here actually they are not inertial anymore due to the rotation of the frame S_P. We will show later that $\boldsymbol{z}$ is suitable for our dynamical modeling.

The non-canonical Hamiltonian structure of this system has a Poisson bracket $\{\cdot,\cdot\}_{\mathbb{R}^{18}}(\boldsymbol{z})$, which can be written in terms of Poisson tensor as

$$\{f, g\}_{\mathbb{R}^{18}}(\boldsymbol{z}) = \left(\nabla_{\boldsymbol{z}} f\right)^T \boldsymbol{B}(\boldsymbol{z}) \left(\nabla_{\boldsymbol{z}} g\right) \tag{3}$$

for any $f, g \in C^{\infty}(\mathbb{R}^{18})$. The Poisson tensor $\boldsymbol{B}(\boldsymbol{z})$ is given by [43]

$$\boldsymbol{B}(\boldsymbol{z}) = \begin{bmatrix} -\hat{\boldsymbol{\Gamma}} & -\hat{\boldsymbol{\alpha}}_a & -\hat{\boldsymbol{\beta}}_a & -\hat{\boldsymbol{\gamma}}_a & \mathbf{0} & \mathbf{0} \\ -\hat{\boldsymbol{\alpha}}_a & \mathbf{0} & \mathbf{0} & \mathbf{0} & \mathbf{0} & \mathbf{0} \\ -\hat{\boldsymbol{\beta}}_a & \mathbf{0} & \mathbf{0} & \mathbf{0} & \mathbf{0} & \mathbf{0} \\ -\hat{\boldsymbol{\gamma}}_a & \mathbf{0} & \mathbf{0} & \mathbf{0} & \mathbf{0} & \mathbf{0} \\ \mathbf{0} & \mathbf{0} & \mathbf{0} & \mathbf{0} & \mathbf{0} & \mathbf{I}_{3\times 3} \\ \mathbf{0} & \mathbf{0} & \mathbf{0} & \mathbf{0} & -\mathbf{I}_{3\times 3} & \mathbf{0} \end{bmatrix}, \tag{4}$$

where $\mathbf{I}_{3\times 3}$ is the 3×3 identity matrix, and the hat map $\hat{}: \mathbb{R}^3 \to so(3)$ is the usual Lie algebra isomorphism and also the cross product matrix. For a vector $\boldsymbol{w} = [w^x, w^y, w^z]^T$, we have

$$\hat{\boldsymbol{w}} = \begin{bmatrix} 0 & -w^z & w^y \\ w^z & 0 & -w^x \\ -w^y & w^x & 0 \end{bmatrix}. \tag{5}$$

The antisymmetric Poisson tensor $\boldsymbol{B}(\boldsymbol{z})$ has six geometric integrals as independent Casimir functions [43]

$$C_1(\boldsymbol{z}) = \frac{1}{2}\boldsymbol{\alpha}_a^T \boldsymbol{\alpha}_a \equiv \frac{1}{2}, C_2(\boldsymbol{z}) = \frac{1}{2}\boldsymbol{\beta}_a^T \boldsymbol{\beta}_a \equiv \frac{1}{2}, C_3(\boldsymbol{z}) = \frac{1}{2}\boldsymbol{\gamma}_a^T \boldsymbol{\gamma}_a \equiv \frac{1}{2}, \tag{6}$$

$$C_4(\boldsymbol{z}) = \boldsymbol{\alpha}_a^T \boldsymbol{\beta}_a \equiv 0, C_5(\boldsymbol{z}) = \boldsymbol{\alpha}_a^T \boldsymbol{\gamma}_a \equiv 0, C_6(\boldsymbol{z}) = \boldsymbol{\beta}_a^T \boldsymbol{\gamma}_a \equiv 0. \tag{7}$$

The twelve-dimensional invariant manifold of the system can be defined in $\mathbb{R}^{18}$ by Casimir functions

$$\Sigma = \left\{ \left(\boldsymbol{\Gamma}^T, \boldsymbol{\alpha}_a^T, \boldsymbol{\beta}_a^T, \boldsymbol{\gamma}_a^T, \boldsymbol{r}^T, \boldsymbol{p}^T \right)^T \in \mathbb{R}^{18} \mid C_1(\boldsymbol{z}) = C_2(\boldsymbol{z}) = C_3(\boldsymbol{z}) = \frac{1}{2}, C_4(\boldsymbol{z}) = C_5(\boldsymbol{z}) = C_6(\boldsymbol{z}) = 0 \right\}, \tag{8}$$

which is the symplectic leaf of the system, on which the restriction of Poisson bracket $\{\cdot,\cdot\}_{\mathbb{R}^{18}}(\boldsymbol{z})$ defines the symplectic structure.

According to Ref. [38], the Hamiltonian is written in terms of $\boldsymbol{z}$ as

$$H(\boldsymbol{z}) = \frac{1}{2}\boldsymbol{\Gamma}^T \boldsymbol{A}\boldsymbol{I}^{-1}\boldsymbol{A}^T \boldsymbol{\Gamma} + \frac{|\boldsymbol{p}|^2}{2m} + V(\boldsymbol{z}) - \omega_T \boldsymbol{\Gamma}^T \boldsymbol{e}_3 - \omega_T \boldsymbol{p}^T \left(\hat{\boldsymbol{e}}_3 \boldsymbol{r}\right), \tag{9}$$

where m and $\boldsymbol{I} = diag\left\{I_{xx}, I_{yy}, I_{zz}\right\}$ are the mass and inertia tensor of spacecraft, respectively, $V(\boldsymbol{z})$ is the gravitational potential, and $\boldsymbol{e}_3 = \left[0, 0, 1\right]^T$.

With $\boldsymbol{B}(\boldsymbol{z})$ and $H(\boldsymbol{z})$, the equations of motion can be written in the Hamiltonian form

$$\dot{\boldsymbol{z}} = \boldsymbol{B}(\boldsymbol{z}) \nabla_{\boldsymbol{z}} H(\boldsymbol{z}). \tag{10}$$

The explicit equations of 6-DOF orbit-attitude motion expressed in the body-fixed frame of the asteroid S_P can be obtained from Eqs. (4), (9), and (10) as follows:

$$
\begin{aligned}
\begin{bmatrix} \dot{\boldsymbol{\Gamma}} \\ \dot{\boldsymbol{\alpha}}_a \\ \dot{\boldsymbol{\beta}}_a \\ \dot{\boldsymbol{\gamma}}_a \\ \dot{\boldsymbol{r}} \\ \dot{\boldsymbol{p}} \end{bmatrix} &= \begin{bmatrix} -\hat{\boldsymbol{\Gamma}} & -\hat{\boldsymbol{\alpha}}_a & -\hat{\boldsymbol{\beta}}_a & -\hat{\boldsymbol{\gamma}}_a & \mathbf{0} & \mathbf{0} \\ -\hat{\boldsymbol{\alpha}}_a & \mathbf{0} & \mathbf{0} & \mathbf{0} & \mathbf{0} & \mathbf{0} \\ -\hat{\boldsymbol{\beta}}_a & \mathbf{0} & \mathbf{0} & \mathbf{0} & \mathbf{0} & \mathbf{0} \\ -\hat{\boldsymbol{\gamma}}_a & \mathbf{0} & \mathbf{0} & \mathbf{0} & \mathbf{0} & \mathbf{0} \\ \mathbf{0} & \mathbf{0} & \mathbf{0} & \mathbf{0} & \mathbf{0} & \mathbf{I}_{3\times 3} \\ \mathbf{0} & \mathbf{0} & \mathbf{0} & \mathbf{0} & -\mathbf{I}_{3\times 3} & \mathbf{0} \end{bmatrix} \begin{bmatrix} \boldsymbol{A}\boldsymbol{I}^{-1}\boldsymbol{A}^T\boldsymbol{\Gamma} - \omega_T \boldsymbol{e}_3 \\ (\boldsymbol{\Gamma}\cdot\boldsymbol{\alpha}_a)\boldsymbol{\Gamma}/I_{xx} + \partial V/\partial \boldsymbol{\alpha}_a \\ (\boldsymbol{\Gamma}\cdot\boldsymbol{\beta}_a)\boldsymbol{\Gamma}/I_{yy} + \partial V/\partial \boldsymbol{\beta}_a \\ (\boldsymbol{\Gamma}\cdot\boldsymbol{\gamma}_a)\boldsymbol{\Gamma}/I_{zz} + \partial V/\partial \boldsymbol{\gamma}_a \\ -\omega_T \hat{\boldsymbol{p}}\boldsymbol{e}_3 + \partial V/\partial \boldsymbol{r} \\ \omega_T \hat{\boldsymbol{r}}\boldsymbol{e}_3 + \boldsymbol{p}/m \end{bmatrix} \\
&= \begin{bmatrix} \left\{ -\hat{\boldsymbol{\Gamma}}\left(\boldsymbol{A}\boldsymbol{I}^{-1}\boldsymbol{A}^T\boldsymbol{\Gamma} - \omega_T\boldsymbol{e}_3\right) - \hat{\boldsymbol{\alpha}}_a\left[(\boldsymbol{\Gamma}\cdot\boldsymbol{\alpha}_a)\boldsymbol{\Gamma}/I_{xx} + \partial V/\partial\boldsymbol{\alpha}_a\right] \right. \\ \left. -\hat{\boldsymbol{\beta}}_a\left[(\boldsymbol{\Gamma}\cdot\boldsymbol{\beta}_a)\boldsymbol{\Gamma}/I_{yy} + \partial V/\partial\boldsymbol{\beta}_a\right] - \hat{\boldsymbol{\gamma}}_a\left[(\boldsymbol{\Gamma}\cdot\boldsymbol{\gamma}_a)\boldsymbol{\Gamma}/I_{zz} + \partial V/\partial\boldsymbol{\gamma}_a\right] \right\} \\ \hat{\boldsymbol{\alpha}}_a\left(\omega_T\boldsymbol{e}_3 - \boldsymbol{A}\boldsymbol{I}^{-1}\boldsymbol{A}^T\boldsymbol{\Gamma}\right) \\ \hat{\boldsymbol{\beta}}_a\left(\omega_T\boldsymbol{e}_3 - \boldsymbol{A}\boldsymbol{I}^{-1}\boldsymbol{A}^T\boldsymbol{\Gamma}\right) \\ \hat{\boldsymbol{\gamma}}_a\left(\omega_T\boldsymbol{e}_3 - \boldsymbol{A}\boldsymbol{I}^{-1}\boldsymbol{A}^T\boldsymbol{\Gamma}\right) \\ \omega_T\hat{\boldsymbol{r}}\boldsymbol{e}_3 + \boldsymbol{p}/m \\ \omega_T\hat{\boldsymbol{p}}\boldsymbol{e}_3 - \partial V/\partial\boldsymbol{r} \end{bmatrix} \\
&= \begin{bmatrix} \omega_T\hat{\boldsymbol{\Gamma}}\boldsymbol{e}_3 - \hat{\boldsymbol{\alpha}}_a\left(\partial V/\partial\boldsymbol{\alpha}_a\right) - \hat{\boldsymbol{\beta}}_a\left(\partial V/\partial\boldsymbol{\beta}_a\right) - \hat{\boldsymbol{\gamma}}_a\left(\partial V/\partial\boldsymbol{\gamma}_a\right) \\ -\hat{\boldsymbol{\alpha}}_a\left(\boldsymbol{A}\boldsymbol{I}^{-1}\boldsymbol{A}^T\boldsymbol{\Gamma} - \omega_T\boldsymbol{e}_3\right) \\ -\hat{\boldsymbol{\beta}}_a\left(\boldsymbol{A}\boldsymbol{I}^{-1}\boldsymbol{A}^T\boldsymbol{\Gamma} - \omega_T\boldsymbol{e}_3\right) \\ -\hat{\boldsymbol{\gamma}}_a\left(\boldsymbol{A}\boldsymbol{I}^{-1}\boldsymbol{A}^T\boldsymbol{\Gamma} - \omega_T\boldsymbol{e}_3\right) \\ \omega_T\hat{\boldsymbol{r}}\boldsymbol{e}_3 + \boldsymbol{p}/m \\ \omega_T\hat{\boldsymbol{p}}\boldsymbol{e}_3 - \partial V/\partial\boldsymbol{r} \end{bmatrix}.
\end{aligned}
\tag{11}
$$

At the right-hand side of Eq. (11), the terms $\omega_T\hat{\boldsymbol{\Gamma}}\boldsymbol{e}_3$, $\omega_T\hat{\boldsymbol{r}}\boldsymbol{e}_3$, and $\omega_T\hat{\boldsymbol{p}}\boldsymbol{e}_3$ are introduced by the uniform rotation of the asteroid frame S_P, and the term $\boldsymbol{A}\boldsymbol{I}^{-1}\boldsymbol{A}^T\boldsymbol{\Gamma} - \omega_T\boldsymbol{e}_3$ is the relative angular velocity of the spacecraft with respect to the asteroid expressed in the asteroid frame S_P. According to Eq. (11), the gravitational force $\boldsymbol{f}$ and gravity gradient torque $\boldsymbol{T}_a$ acting on the spacecraft expressed in the body-fixed frame of the asteroid S_P can be written in terms of derivatives of the gravitational potential $V(\boldsymbol{r}, \boldsymbol{\alpha}_a, \boldsymbol{\beta}_a, \boldsymbol{\gamma}_a)$ as follows

$$
\begin{cases} \boldsymbol{f} = -\dfrac{\partial V(\boldsymbol{r}, \boldsymbol{\alpha}_a, \boldsymbol{\beta}_a, \boldsymbol{\gamma}_a)}{\partial \boldsymbol{r}}, \\ \boldsymbol{T}_a = -\boldsymbol{\alpha}_a \times \dfrac{\partial V(\boldsymbol{r}, \boldsymbol{\alpha}_a, \boldsymbol{\beta}_a, \boldsymbol{\gamma}_a)}{\partial \boldsymbol{\alpha}_a} - \boldsymbol{\beta}_a \times \dfrac{\partial V(\boldsymbol{r}, \boldsymbol{\alpha}_a, \boldsymbol{\beta}_a, \boldsymbol{\gamma}_a)}{\partial \boldsymbol{\beta}_a} - \boldsymbol{\gamma}_a \times \dfrac{\partial V(\boldsymbol{r}, \boldsymbol{\alpha}_a, \boldsymbol{\beta}_a, \boldsymbol{\gamma}_a)}{\partial \boldsymbol{\gamma}_a}. \end{cases}
\tag{12}
$$

Gravitational Potential, Force, and Torque

The last step to finalize the dynamical modeling process is to obtain the expression of the gravitational potential $V(\boldsymbol{r}, \boldsymbol{\alpha}_a, \boldsymbol{\beta}_a, \boldsymbol{\gamma}_a)$ and expressions of the gravitational force $\boldsymbol{f}$ and gravity gradient torque $\boldsymbol{T}_a$ further by using Eq. (12). Our gravitational model proposed for the binary asteroid system in Ref. [25] will be adopted.

The asteroid is considered as a homogeneous polyhedron and its gravity can be described in a closed form via the approach by Werner and Scheeres [26]. The surface of the polyhedron consists of triangular faces with mutual vertexes and edges, and the polyhedron can be

defined by coordinates of the vertexes and the triads of vertexes that determine the triangular faces.

The force potential, i.e., the minus gravitational potential, of a field point with position vector $\boldsymbol{r}_p$ in the asteroid body-fixed frame S_P is given by

$$U(\boldsymbol{r}_p)=\frac{1}{2}G\sigma\left(\sum_{e\in edges}L_e\boldsymbol{r}_e^T\boldsymbol{E}_e\boldsymbol{r}_e-\sum_{f\in faces}\omega_f\boldsymbol{r}_f^T\boldsymbol{F}_f\boldsymbol{r}_f\right), \tag{13}$$

and its derivatives are given by

$$\nabla U(\boldsymbol{r}_p)=-G\sigma\left(\sum_{e\in edges}L_e\boldsymbol{E}_e\boldsymbol{r}_e-\sum_{f\in faces}\omega_f\boldsymbol{F}_f\boldsymbol{r}_f\right), \tag{14}$$

$$\nabla\nabla U(\boldsymbol{r}_p)=G\sigma\left(\sum_{e\in edges}L_e\boldsymbol{E}_e-\sum_{f\in faces}\omega_f\boldsymbol{F}_f\right), \tag{15}$$

where G is the gravitational constant, σ is the density of the polyhedron, $\boldsymbol{E}_e$ and $\boldsymbol{F}_f$ are geometric parameters denoted as 3×3 matrices, $\boldsymbol{r}_e$ and $\boldsymbol{r}_f$ are vectors from the field point to any point on the edge and face of the polyhedron expressed in the asteroid body-fixed frame S_P, respectively. L_e is defined as

$$L_e=\mathrm{In}(a+b+e)-\mathrm{In}(a+b-e), \tag{16}$$

where a, b, and e are distances from the field point to the edge's two ends and the edge length, respectively, as shown in Fig. 2.

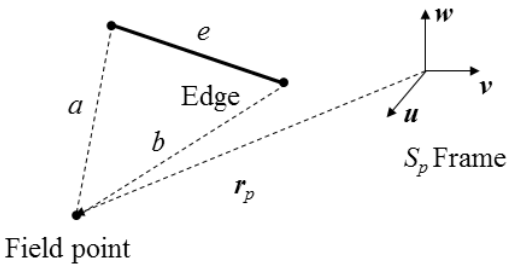

Fig. 2: Parameters about L_e

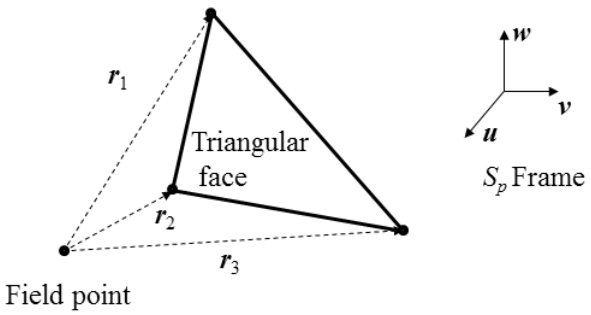

Fig. 3: Parameters about ω_f

ω_f is defined as

$$\omega_f=2\arctan\left(\frac{N}{M}\right), \tag{17}$$

$$M=r_1r_2r_3+r_1(\boldsymbol{r}_2\cdot\boldsymbol{r}_3)+r_2(\boldsymbol{r}_3\cdot\boldsymbol{r}_1)+r_3(\boldsymbol{r}_1\cdot\boldsymbol{r}_2), \tag{18}$$

$$N=\boldsymbol{r}_1\cdot(\boldsymbol{r}_2\times\boldsymbol{r}_3), \tag{19}$$

where $\boldsymbol{r}_1$, $\boldsymbol{r}_2$, and $\boldsymbol{r}_3$ are vectors from the field point to the three vertexes of the triangular face, whose 1-2-3 order is in the right-hand order around the outward-pointing normal vector, as shown in Fig. 3. More details about the gravitational model of a homogeneous polyhedron can be found in Ref. [26].

The gravitational potential of the extended, rigid spacecraft is the volume integration of the gravitational potential $-U(\boldsymbol{r}_p)$ over the spacecraft

$$V(\boldsymbol{r}, \boldsymbol{\alpha}_a, \boldsymbol{\beta}_a, \boldsymbol{\gamma}_a) = \int_B -U(\boldsymbol{r}_p)\, dm\,, \tag{20}$$

the second-order approximation of which can be written in terms of relative position $\boldsymbol{r}$, relative attitude $\boldsymbol{\alpha}_a$, $\boldsymbol{\beta}_a$, and $\boldsymbol{\gamma}_a$, and the moments of inertia of the spacecraft [25]

$$\begin{aligned} V(\boldsymbol{r}, \boldsymbol{\alpha}_a, \boldsymbol{\beta}_a, \boldsymbol{\gamma}_a) &= -U(\boldsymbol{r})m - \frac{1}{2}\left[J_{xx}\boldsymbol{\alpha}_a^T \nabla\nabla U(\boldsymbol{r})\boldsymbol{\alpha}_a + J_{yy}\boldsymbol{\beta}_a^T \nabla\nabla U(\boldsymbol{r})\boldsymbol{\beta}_a + J_{zz}\boldsymbol{\gamma}_a^T \nabla\nabla U(\boldsymbol{r})\boldsymbol{\gamma}_a\right] \\ &= -U(\boldsymbol{r})m - \frac{1}{2}G\sigma\left[J_{xx}\boldsymbol{\alpha}_a^T\left(\sum_{e\in edges} L_e \boldsymbol{E}_e - \sum_{f\in faces}\omega_f \boldsymbol{F}_f\right)\boldsymbol{\alpha}_a\right. \\ &\quad \left. + J_{yy}\boldsymbol{\beta}_a^T\left(\sum_{e\in edges} L_e \boldsymbol{E}_e - \sum_{f\in faces}\omega_f \boldsymbol{F}_f\right)\boldsymbol{\beta}_a + J_{zz}\boldsymbol{\gamma}_a^T\left(\sum_{e\in edges} L_e \boldsymbol{E}_e - \sum_{f\in faces}\omega_f \boldsymbol{F}_f\right)\boldsymbol{\gamma}_a\right], \end{aligned} \tag{21}$$

where the second-order mass distribution parameters J_{xx}, J_{yy}, and J_{zz} are defined in terms of moments of inertia

$$J_{xx} = \frac{1}{2}\left(-I_{xx} + I_{yy} + I_{zz}\right),\ J_{yy} = \frac{1}{2}\left(I_{xx} - I_{yy} + I_{zz}\right),\ J_{zz} = \frac{1}{2}\left(I_{xx} + I_{yy} - I_{zz}\right). \tag{22}$$

The gravitational force $\boldsymbol{f}$ and gravity gradient torque $\boldsymbol{T}_a$ acting on the spacecraft can be derived by using Eq. (12)

$$\begin{aligned} \boldsymbol{f} &= \nabla U(\boldsymbol{r})m + \frac{1}{2}G\sigma\left[J_{xx}\left(\sum_{e\in edges}\boldsymbol{\alpha}_a^T \boldsymbol{E}_e \boldsymbol{\alpha}_a \nabla L_e - \sum_{f\in faces}\boldsymbol{\alpha}_a^T \boldsymbol{F}_f \boldsymbol{\alpha}_a \nabla\omega_f\right)\right. \\ &\quad \left. + J_{yy}\left(\sum_{e\in edges}\boldsymbol{\beta}_a^T \boldsymbol{E}_e \boldsymbol{\beta}_a \nabla L_e - \sum_{f\in faces}\boldsymbol{\beta}_a^T \boldsymbol{F}_f \boldsymbol{\beta}_a \nabla\omega_f\right) + J_{zz}\left(\sum_{e\in edges}\boldsymbol{\gamma}_a^T \boldsymbol{E}_e \boldsymbol{\gamma}_a \nabla L_e - \sum_{f\in faces}\boldsymbol{\gamma}_a^T \boldsymbol{F}_f \boldsymbol{\gamma}_a \nabla\omega_f\right)\right], \end{aligned} \tag{23}$$

$$\boldsymbol{T}_a = J_{xx}\boldsymbol{\alpha}_a \times \nabla\nabla U(\boldsymbol{r})\boldsymbol{\alpha}_a + J_{yy}\boldsymbol{\beta}_a \times \nabla\nabla U(\boldsymbol{r})\boldsymbol{\beta}_a + J_{zz}\boldsymbol{\gamma}_a \times \nabla\nabla U(\boldsymbol{r})\boldsymbol{\gamma}_a\,, \tag{24}$$

where the explicit expressions of ∇L_e and $\nabla\omega_f$ are referred to Ref. [25].

Model Analyses via Numerical Simulations

The model analyses will be carried out by comparing with the point-mass/spherical gravity and the harmonic gravity, to see the improvements of the polyhedron gravity in the modeling of the gravitationally coupled orbit-attitude motion.

The asteroid 6489 Golevka will be considered. Its shape model with 2048 vertexes and 4092 triangular faces can be obtained from the NASA database, as shown in Fig. 4. The density of the asteroid is 2700 kg/m^3. The angular velocity of its uniform rotation is $\omega_T = 2.8963\times10^{-4}\,\mathrm{s}^{-1}$.

The parameters of the harmonic gravity are calculated from the shape model to ensure that the gravity models are of the exactly the same asteroid. The harmonic gravity parameters are:

$$\mu = 14.0374\ \mathrm{m}^3/\mathrm{s}^2,\ C_{20} = -0.0712,\ C_{22} = -0.0332,\ a_e = 265\ \mathrm{m}, \tag{25}$$

where C_{20} and C_{22} are the second degree and order harmonic coefficients, and a_e is the mean radius of the asteroid. The spherical gravity can be obtained by simply letting C_{20}=C_{22}=0. The gravitationally coupled orbit-attitude dynamical models with the spherical gravity and harmonic gravity are referred to Ref. [44].

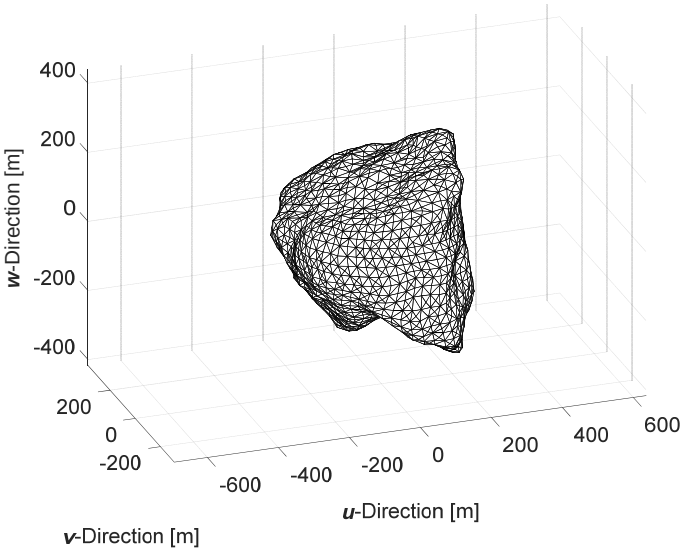

Fig. 4: Shape of the asteroid 6489 Golevka

The parameters of spacecraft are chosen as

$$m = 1\times 10^3 \text{ kg}, \ \boldsymbol{I} = \begin{bmatrix} 2 & 0 & 0 \\ 0 & 1 & 0 \\ 0 & 0 & 1.6 \end{bmatrix} \times 10^3 \text{ kg}\cdot\text{m}^2 . \tag{26}$$

The initial relative configuration of spacecraft with respect to the asteroid is chosen as

$$\boldsymbol{A}_0 = \begin{bmatrix} \cos(\frac{\pi}{9}) & -\sin(\frac{\pi}{9}) & 0 \\ \sin(\frac{\pi}{9}) & \cos(\frac{\pi}{9}) & 0 \\ 0 & 0 & 1 \end{bmatrix} \begin{bmatrix} \cos(-\frac{\pi}{20}) & 0 & \sin(-\frac{\pi}{20}) \\ 0 & 1 & 0 \\ -\sin(-\frac{\pi}{20}) & 0 & \cos(-\frac{\pi}{20}) \end{bmatrix} \begin{bmatrix} 1 & 0 & 0 \\ 0 & \cos(\frac{\pi}{18}) & -\sin(\frac{\pi}{18}) \\ 0 & \sin(\frac{\pi}{18}) & \cos(\frac{\pi}{18}) \end{bmatrix}, \tag{27}$$

$$\boldsymbol{r}_0 = \left[400, 0, 0\right]^T \text{m} . \tag{28}$$

The initial relative velocity of the spacecraft with respect to the asteroid expressed in the spacecraft body-fixed frame is chosen as

$$\begin{bmatrix} \boldsymbol{\Omega}_{R0} \\ \boldsymbol{V}_{R0} \end{bmatrix} = \left[0\ \text{s}^{-1}, \quad 0\ \text{s}^{-1}, \quad 0\ \text{s}^{-1}, \quad -0.1\ \text{m/s}, \quad 0.2\ \text{m/s}, \quad 0.15\ \text{m/s}\right]^T \tag{29}$$

where the definition of the relative velocity is referred to Ref. [44].

The attitude error and position error of the harmonic gravity and spherical gravity compared with the proposed polyhedron gravity are shown in Figs. 5 and 6, respectively. The attitude error is described by the principal rotation vector $\boldsymbol{\Theta}_e$ of the error attitude matrix $\boldsymbol{A}_e$ and its norm $\phi = |\boldsymbol{\Theta}_e|$, while the position error is described by the position difference $\boldsymbol{r}_e$ in the asteroid body-fixed frame and its norm r_e.

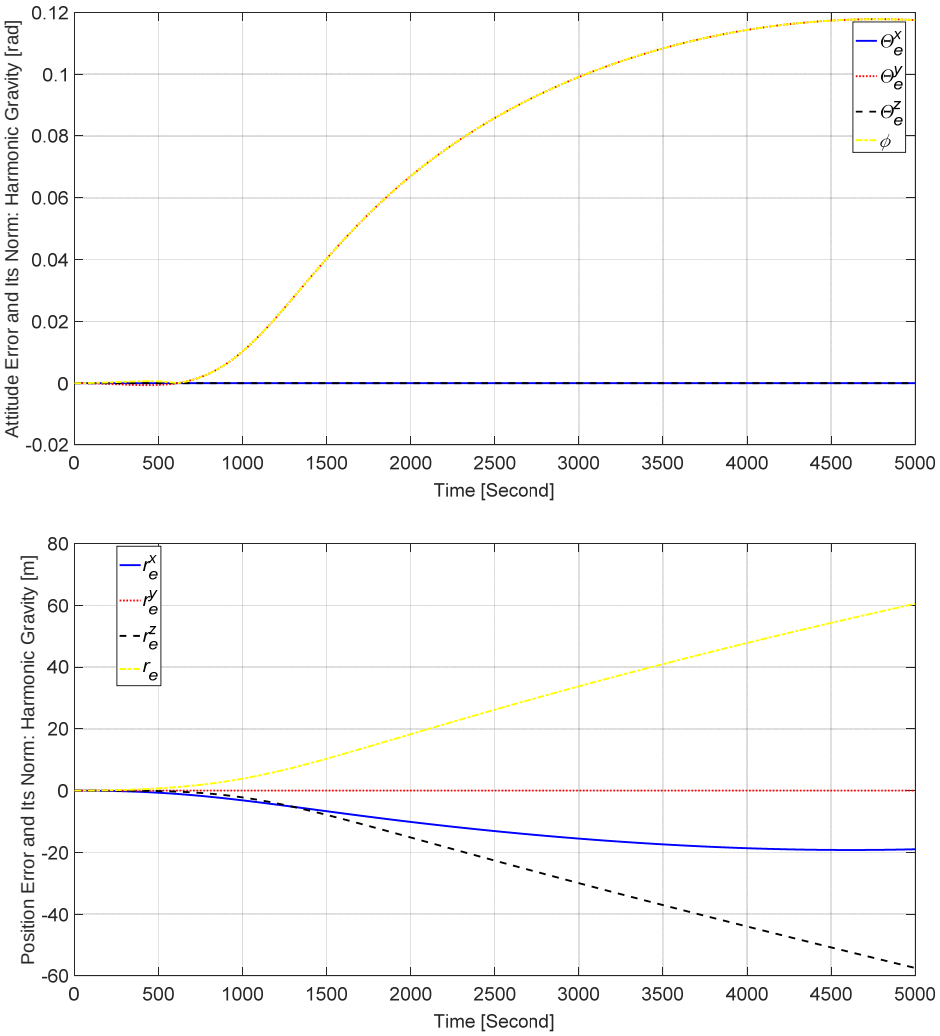

Fig. 5: Attitude error and position error of harmonic gravity

The trajectories of the spacecraft's center of mass in the asteroid body-fixed frame with three different gravity models are shown in Fig. 7, where several snapshots of the attitude of the spacecraft are also shown.

It has been shown that after 5000 seconds, both the harmonic gravity and spherical gravity have significant errors compared with the proposed polyhedron gravity. The spherical gravity has a position error of 100 m and an attitude error of 0.15 rad (8.59 degree), while the harmonic gravity has a better performance, with a position error of 60 m and an attitude error of 0.12 rad (6.88 degree).

Therefore, the irregularity of the asteroid gravity has significant effects on the gravitationally coupled orbit-attitude dynamics, and cannot be precisely described by the harmonic series. The proposed model with the gravity of a homogeneous polyhedron in this paper is necessary and provides a high-precision description for the coupled orbit-attitude motion in the close proximity of a small, irregular-shaped asteroid.

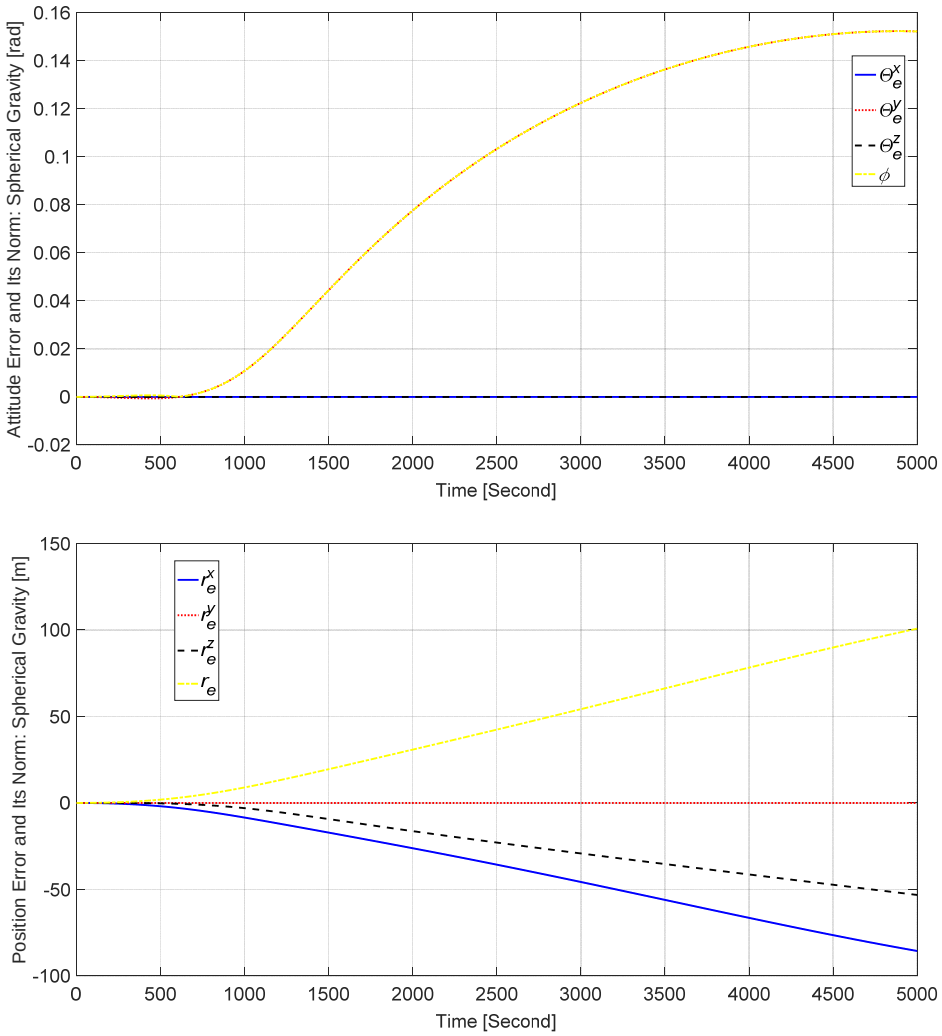

Fig. 6: Attitude error and position error of spherical gravity

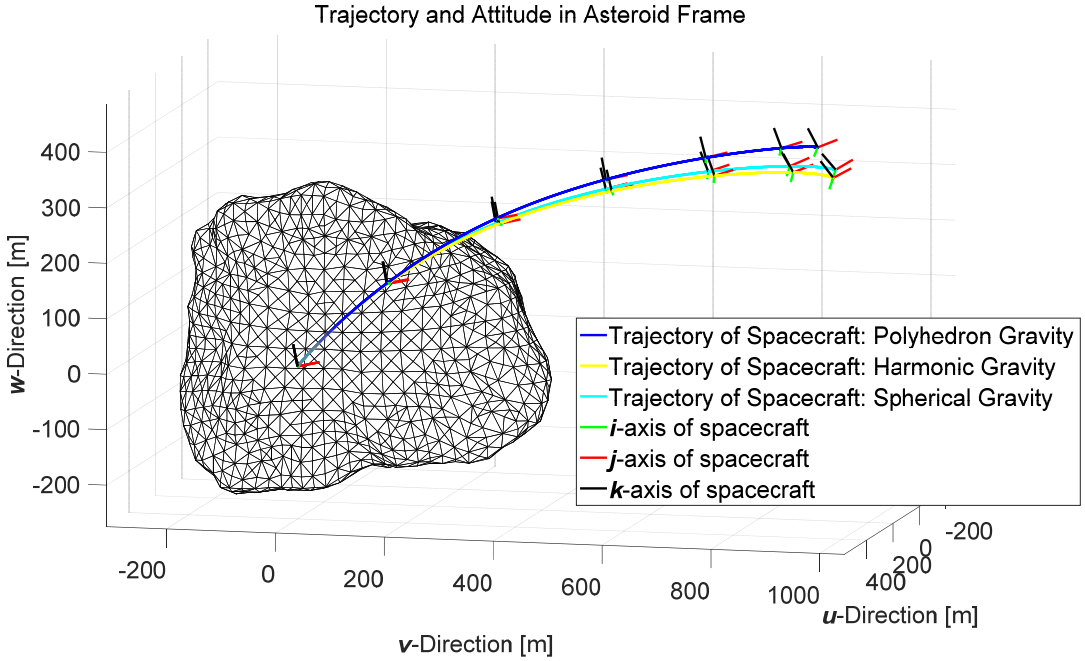

Fig. 7: Trajectories and attitudes of the spacecraft in the asteroid body-fixed frame with three different gravity models

Conclusion

The gravitationally coupled orbit-attitude dynamics of a rigid spacecraft about an irregular-shaped asteroid has been established by using a newly proposed gravitational potential model and the non-canonical Hamiltonian structure of the problem. In the gravitational model, the gravity field of the asteroid is modelled as that of a homogeneous polyhedron, so that the irregular gravity field can be fully modeled without discarding higher-order terms, enabling a high precision even near the asteroid's surface. The gravitational potential is finally written in terms of moments of inertia of the spacecraft, and the gravitational force and gravity gradient torque are derived by means of derivatives of the potential. The dynamical model has been analyzed by comparing with models with the point-mass/spherical gravity and the harmonic gravity, to see effects of irregularity of the asteroid's gravity. Results have shown that the irregularity of gravity has significant effects on the coupled orbit-attitude dynamics, and cannot be described satisfactorily by the existing model with harmonic series.

Acknowledgments

This work has been supported by the National Natural Science Foundation of China under Grants 11432001, 11602009, and 11872007, the Young Elite Scientist Sponsorship Program by China Association for Science and Technology, and the Fundamental Research Funds for the Central Universities.

References

1. Kinoshita, H. Stationary motions of an axisymmetric body around a spherical body and their stability. Publ. Astron. Soc. Jpn. 22, 383–403, 1970.
2. Kinoshita, H. Stationary motions of a triaxial body and their stability. Publ. Astron. Soc. Jpn. 24, 409–417, 1972a.
3. Kinoshita, H. First-order perturbations of the two finite body problem. Publ. Astron. Soc. Jpn. 24, 423–457, 1972b.
4. Beletskii, V.V., Ponomareva, O.N. A parametric analysis of relative equilibrium stability in a gravitational field. Kosm. Issled. 28(5), 664–675, 1990.
5. Maciejewski, A.J. Reduction, relative equilibria and potential in the two rigid bodies problem. Celest. Mech. Dyn. Astron. 63, 1–28, 1995.
6. Scheeres, D.J. Stability in the full two-body problem. Celest. Mech. Dyn. Astron. 83, 155–169, 2002.
7. Scheeres, D.J. Stability of relative equilibria in the full two-body problem. Ann. N. Y. Acad. Sci. 1017, 81–94, 2004.
8. Scheeres, D.J. Stability of the planar full 2-body problem. Celest. Mech. Dyn. Astron. 104, 103–128, 2009.
9. Koon, W.-S., Marsden, J.E., Ross, S.D., Lo, M., Scheeres, D.J. Geometric mechanics and the dynamics of asteroid pairs. Ann. N. Y. Acad. Sci. 1017, 11–38, 2004.
10. Bellerose, J., Scheeres, D.J. Energy and stability in the full two body problem. Celest. Mech. Dyn. Astron. 100, 63–91, 2008.
11. Boué, G., Laskar, J. Spin axis evolution of two interacting bodies. Icarus 201, 750–767, 2009.
12. Ćuk, M., Nesvorný, D. Orbital evolution of small binary asteroids. Icarus 207, 732-743 (2010)
13. McMahon, J.W., Scheeres, D.J. Dynamic limits on planar libration-orbit coupling around an oblate primary. Celest. Mech. Dyn. Astron. 115, 365–396, 2013.

14. Schutz, B.E.: The mutual potential and gravitational torque of two bodies to fourth order. Celest. Mech. 24, 173–181 (1981)
15. Ashenberg, J.: Mutual gravitational potential and torque of solid bodies via inertia integrals. Celest. Mech. Dyn. Astron. 99, 149–159 (2007)
16. Tricarico, P., Figure-figure interaction between bodies having arbitrary shapes and mass distributions: a power series expansion approach. Celestial Mechanics and Dynamical Astronomy, 100(4), 319-330 (2008)
17. Giacaglia, C.E., Jefferys, W.H.: Motion of a space station. Celest. Mech. 4, 442–467 (1971)
18. Borderies, N.: Mutual gravitational potential of N solid bodies. Celest. Mech. 18, 173–181 (1978)
19. Boué G. The two rigid body interaction using angular momentum theory formulae. Celestial Mechanics and Dynamical Astronomy, 128(2-3): 261-273 (2017)
20. Werner, R.A., Scheeres, D.J., Mutual potential of homogeneous polyhedra, Celestial Mechanics and Dynamical Astronomy, vol. 91, pp. 337-349 (2005)
21. Fahnestock, E.G., Scheeres, D.J., Simulation and analysis of the dynamics of binary near-Earth Asteroid (66391) 1999 KW4. Icarus 194, 410-435 (2008)
22. Hirabayashi, M., and Scheeres, D. J., Recursive computation of mutual potential between two polyhedra, Celestial Mechanics and Dynamical Astronomy, vol. 117, pp. 245-262 (2013)
23. Hou, X., Scheeres, D.J. , and Xin, X., Mutual potential between two rigid bodies with arbitrary shapes and mass distributions. Celestial Mechanics and Dynamical Astronomy, 127(3): 369-395 (2017)
24. Compère, A., Lemaître A., The two-body interaction potential in the STF tensor formalism: an application to binary asteroids. Celestial Mechanics and Dynamical Astronomy, 119(3-4), 313-330 (2014)
25. Shi, Y., Wang, Y., Xu, S., Mutual gravitational potential, force, and torque of a homogeneous polyhedron and an extended body: an application to binary asteroids, Celest. Mech. Dyn. Astron. 129(3), 307–320 (2017)
26. Werner, R.A., Scheeres, D.J., Exterior gravitation of a polyhedron derived and compared with harmonic and mascon gravitation representations of asteroid 4769 Castalia, Celestial Mechanics and Dynamical Astronomy, vol. 65, pp. 313-344 (1997)
27. Beletskii V. V.. Motion of an Artificial Satellite About Its Center of Mass, Series: Mechanics of Space Flight, Translated from Russian. Published for the National Aeronautics and Space Administration, USA and the National Science Foundation, Washington, D.C. by the Israel Program for Scientific Translations, 1965
28. Lange B. O.. Linear coupling between orbital and attitude motions of a rigid body. Journal of the Astronautical Sciences, 1970, 18(3): 150–167
29. Mohan S. N., Breakwell J. V., Lange, B. O.. Interaction between attitude libration and orbital motion of a rigid body in a near Keplerian orbit of low eccentricity. Celestial Mechanics, 1972, 5: 157–173
30. Sincarsin G. B., Hughes P. C.. Gravitational orbit-attitude coupling for very large spacecraft. Celestial Mechanics, 1983, 31: 143–161
31. Zanardi M. C.. Study of the terms of coupling between rotational and translational motions. Celestial Mechanics, 1986, 39: 147–158
32. Wang, Y., Xu, S.: Gravitational orbit-rotation coupling of a rigid satellite around a spheroid planet. J. Aerosp. Eng. 27(1), 140–150 (2014a)
33. Scheeres, D.J. Spacecraft at small NEO. arXiv: physics/0608158v1, 2006.
34. Wang, Y., Xu, S.: Symmetry, reduction and relative equilibria of a rigid body in the J_2 problem. Adv. Space Res. 51(7), 1096–1109 (2013a)

35. Wang, Y., Xu, S.: Stability of the classical type of relative equilibria of a rigid body in the J_2 problem. Astrophys. Space Sci. 346(2), 443–461 (2013b)
36. Wang, Y., Xu, S., Tang, L.: On the existence of the relative equilibria of a rigid body in the J_2 problem. Astrophys. Space Sci. 353(2), 425–440 (2014a)
37. Wang, Y., Xu, S.: Relative equilibria of full dynamics of a rigid body with gravitational orbit-attitude coupling in a uniformly rotating second degree and order gravity field. Astrophys. Space Sci. 354(2), 339–353 (2014b)
38. Wang, Y., Xu, S., Zhu, M.: Stability of relative equilibria of the full spacecraft dynamics around an asteroid with orbit-attitude coupling. Adv. Space Res. 53(7), 1092-1107 (2014b)
39. Kikuchi, S., Howell, K.C., Tsuda, Y., Kawaguchi, J. Orbit-attitude coupled motion around small bodies: sun-synchronous orbits with sun-tracking attitude motion, Acta Astronautica, 140, 34–48, 2017.
40. Lee, D., Sanyal, A.K., Butcher, E.A., Scheeres, D.J.: Almost global asymptotic tracking control for spacecraft body-fixed hovering over an asteroid. Aerosp. Sci. Technol. 38, 105–115 (2014)
41. Misra, G., Izadi, M., Sanyal, A.K., Scheeres, D.J.: Coupled orbit-attitude dynamics and pose estimation of spacecraft near small solar system bodies. Adv. Space Res. 57(8), 1747–1761 (2016)
42. Li, X., Warier, R.R., Sanyal, A.K., Qiao, D.: Trajectory tracking near small bodies using only attitude control. Journal of Guidance, Control, and Dynamics, Vol. 42, No. 1, pp. 109–122 (2019)
43. Wang, Y., Xu, S.: Hamiltonian structures of dynamics of a gyrostat in a gravitational field. Nonlinear Dyn. 70(1), 231–247 (2012)
44. Jiang, L., Wang, Y., Xu, S.: Integrated 6-DOF orbit-attitude dynamical modeling and control using geometric mechanics, International Journal of Aerospace Engineering, Volume 2017, Article ID 4034328, 1–13 (2017)